Picosecond time-resolved fluorescence spectroscopy of K-590 in the bacteriorhodopsin photocycle

G. H. Atkinson, D. Blanchard, H. Lemaire, T. L. Brack, and H. Hayashi
Department of Chemistry and Optical Sciences Center, University of Arizona, Tucson, Arizona 85721

ABSTRACT The fluorescence spectrum of a distinct isomeric and conformational intermediate formed on the 10^{-11} s time scale during the bacteriorhodopsin (BR) photocycle is observed at room temperature using a two laser, pump-probe technique with picosecond time resolution. The BR photocycle is initiated by pulsed (8 ps) excitation at 565 nm, whereas the fluorescence is generated by 4-ps laser pulses at 590 nm. The unstructured fluorescence extends from 650 to 880 nm and appears in the same general spectral region as the fluorescence spectrum assigned to BR-570. The transient fluorescence spectrum can be distinguished from that assigned to BR-570 by a larger emission quantum yield (approximately twice that of BR-570) and by a maximum intensity near 731 nm (shifted 17 nm to higher energy from the maximum of the BR-570 fluorescence spectrum). The fluorescence spectrum of BR-570 only is measured with low energy, picosecond pulsed excitation at 590 nm and is in good agreement with recent data in the literature. The assignment of the transient fluorescence spectrum to the K-590 intermediate is based on its appearance at time delays longer than 40 ps. The K-590 fluorescence spectrum remains unchanged over the entire 40–100-ps interval. The relevance of these fluorescence data with respect to the molecular mechanism used to model the primary processes in the BR photocycle also is discussed.

INTRODUCTION

The identification of photosynthetic activity in bacteriorhodopsin (BR) has focused attention on a biochemical mechanism which appears to function differently from the photosynthetic systems containing chlorophyll (1, 2). Specifically, BR appears to generate a transmembrane chemical potential without the involvement of oxidation-reduction processes (3, 4). Since the subsequent proton and ion transport across the purple membrane containing BR is utilized efficiently in ATP synthesis, considerable attention has been given to the molecular mechanism by which BR utilizes absorbed light energy directly in the formation of a proton gradient across the *Halobacterium halobium* membrane. The molecular processes underlying biochemical activity in BR may provide insight into the molecular dynamics associated with photosynthetic activity in general including other systems containing either retinal or chlorophyll chromophores.

The system under study is composed of three BR moieties arranged with a trimeric structure (5, 6). Each BR contains 248 amino acids, the sequence of which has been determined (7, 8), together with one retinal chromophore. Although the precise molecular contributions of the retinal to the generation of a transmembrane chemical potential remains unresolved, there are several general characteristics describing its molecular transformations which are established. The initial *all-trans* isomer of retinal undergoes changes in configuration, conformation, and protonation during a cyclic set of reactions termed the BR photocycle (9). The absorption of visible light by retinal results in isomerization around the $C_{13}{=}C_{14}$ bond and deprotonation of the Schiff base linkage by which retinal is bound to lysine 216 (9). Time-resolved spectroscopic measurements have determined that deprotonation occurs over a 10^{-5} s time scale (10) while $C_{13}{=}C_{14}$ isomerization appears to begin in the 10^{-12} s time regime (11, 12). The mechanism by which retinal utilizes configurational and conformational changes to convert absorbed light energy into the chemical potential required to drive the photocycle and the associated proton transport is yet to be determined and is the topic of primary interest in this paper.

A variety of spectroscopic techniques has been used to examine the molecular properties of retinal itself and the changes they undergo during the BR photocycle. Orientational properties of the BR-570 have been studied by measuring the circular dichroism associated with the absorption transitions of the retinal chromophore (13). The electronic states populated have been studied extensively by transient absorption spectroscopy (14–24). Time-resolved resonance Raman (TR^3) spectroscopy, developed to measure the vibrational degrees of freedom of transient species (25–30), has been used to examine photocycle transients and thereby to characterize some of the configurational (isomeric) and conformational intermediates of retinal (31, 32). Recently, TR^3 measurements have been extended to the picosecond time regime where the primary processes in the photocycle can be studied (33–38). Emission spectroscopy has been conspic-

0006-3495/89/02/263/12 $2.00

uously absent from this list for several reasons. First, the fluorescence observed with cw excitation is extremely weak and appears as an unstructured band in the 650–880-nm region. This emission has been assigned to fluorescence from stable BR-570 containing retinal in its *all-trans* configuration (39, 40). The weakness of this emission and the relatively low sensitivity of detectors in the near infrared make the measurement of fluorescence difficult experimentally. Second, the absorption spectra of the photocycle intermediates (especially those formed during the initial 100 ps) are strongly overlapped, making it experimentally impractical to excite fluorescence from only one intermediate to the exclusion of others (the M_{412} intermediate may be an exception to this point). Third, the high degree to which BR-570 and the photocycle intermediates are photolytically interconvertible requires that the excitation and probing conditions be quantitatively controlled and optimized separately.

The highly efficient photochemical processes which depopulate excited-state BR ensure that the competitive emission pathways are of low efficiency. Indeed, the initial detection of fluorescence in the BR photocycle not attributable to impurities was reported for a room temperature sample to have a quantum yield of only 10^{-4} (41). Subsequent studies have expanded the characterization of BR fluorescence (24, 42) including its detection in low temperature film samples at 77 K (41, 43–46). Despite these numerous detailed examinations, there remain significant uncertainties concerning even the identity of the emitting species, especially with respect to the contributions of intermediates formed on the picosecond time scale. Although there have been reports of fluorescence from a pseudo BR (P-BR) (43, 46), a recent review has attributed these observations to time-dependent changes in the optical absorbance of the BR sample and concluded that only BR-570 fluoresces in the room temperature samples (39). The same conclusion is reached in studies of 77 K samples (41, 43–46). No fluorescence is assigned to the K-590 intermediate even though an analysis of transient absorption data concludes that a substantial fraction of BR-570 is photolytically converted to a K intermediate (K-625) in 77 K films (47). The observed fluoresence is assigned to BR-570 and characterized with respect to the excited electronic state of BR-570 only (41, 43–46).

The high degree to which the initial molecular processes are photolytically coupled means that variations in the excitation of the sample can greatly complicate the analysis of emission data. This is particularly germane when emission properties of picosecond intermediates are involved. All previous emission studies have used a single laser both to initiate the photocycle and to induce fluorescence. Since the photochemical mixture created during excitation and the emission properties each depends on the spectral and intensity properties of the same laser pulse, it is extremely difficult to deconvolute the resultant data in terms of separate species. To resolve room temperature fluorescence from a picosecond intermediate, the emission from the BR photocycle must be obtained under experimental conditions which emphasize the quantitative control of the photolytic initiation of the photocycle separately from the excitation of fluorescence.

We report in this paper the fluorescence spectrum of an isomerically and conformationally distinct intermediate in the BR photocycle formed within 8 ps of optical excitation at 565 nm. The transient fluorescence signal is larger than that from BR-570 and increases smoothly for delays up to 40 ps before remaining constant for delays at least as long as 100 ps. The fluorescence appears as a broad, unstructured band in the 650–880-nm region which is readily distinguishable from the BR-570 fluorescence spectrum (e.g., the maximum of the transient fluorescence is shifted by 17 nm to higher energy). Comparison of these fluorescence data with results from picosecond and subpicosecond transient absorption (PTA) (17, 18, 21–24) shows that the transient fluorescence originates with the K-590 intermediate. The fluorescence spectrum of BR-570 also is measured under low intensity excitation conditions and is found to agree with results recently reported (24, 42). The time-resolved fluorescence spectroscopy reported here significantly expands our knowledge of the electronic state properties of the K-590 intermediate and provides a new view of the molecular dynamics of the BR photocycle.

EXPERIMENTAL

A. Materials

Purple membrane (PM) is isolated from *Halobacterium halobium* strain R1 by essentially the procedure of Oesterhelt and Stoeckenius (48). Approximately 15 g of cells are suspended in basal salt solution and dialyzed against distilled water overnight. The PM is collected from the dialysate by centrifugation at 100,000 *g* for 30 min and washed by centrifugation with distilled water three times. The membrane is further purified by centrifugation at 140,000 *g* for 15 h on sucrose density gradient. The purple layer above 1.5 M sucrose is collected and centrifuged after being diluted with distilled water. The purified PM is washed three more times by centrifugation, at 100,000 *g* for 30 min, before being suspended in distilled water. The purity of the PM is monitored by the ratios of absorbance (A) at a specific wavelength, A_{280}/A_{565} and A_{700}/A_{565}. The PM sample used for fluorescence measurements exhibits A_{280}/A_{565} = 1.8–2.0 and A_{700}/A_{565} = 0.08–0.1. The pH of the PM suspension is adjusted to 7.0 with dilute NaOH solution and the optical density at 565 nm is adjusted to be 4.0. During the fluorescence measurements, the sample is mechanically degraded (as measured by a decrease of A_{565} and increase of turbidity) due mainly to the circulation through the pump and the jet nozzle (see section B). The laser illumination makes almost no contribution to sample degradation. To minimize the sample degradation, its temperature is kept at ~10°C by cooling the sample reservoir and the pump head with ice water. After ~5

h of experimentation, a 10–30% decrease in A_{565} and an increase in the turbidity of suspension is observed. All the measurements reported here are completed within 2 h.

B. Instrumentation

A schematic representation of the instrumentation for picosecond time-resolved fluorescence (PTRF) and PTA spectroscopy is presented in Fig. 1. The laser system used to provide picosecond pulses for both photochemical and fluorescence excitation consists of two dye lasers (model 703-3; Coherent Inc., Palo Alto, CA) synchronously pumped by the second harmonic output of a cw mode-locked Nd:YAG laser (Quantronix model 416 and SHG model 324). The 532-nm frequency-doubled radiation is produced at a repetition rate of 76 MHz and consists of a train of pulses each of which has a 70-ps (FWHM) duration. The pump radiation is directed into the two dye lasers through a polarizing beam splitter and two half-wave plates which permit the variable division of the power between the dye lasers. The dye laser used to generate fluorescence operates with Rhodamine 6G dye (Exciton) while the dye laser used to optically initiate the BR photocycle operates with a Rhodamine 575 dye (Exciton). The output of each dye laser is controlled by a cavity dumper (model 2200; Coherent Inc.) that is electronically synchronized to the trigger output from the mode-locker used with the Nd:YAG pump laser. This cavity dumper permits the electronic selection of a single picosecond pulse at a chosen frequency.

The output of the dye laser used to either initiate fluorescence or probe the transient absorption is directed to an optical delay line consisting of a quartz corner cube mounted on a translation slide (model B404201J; Velmex, Inc., East Bloomfield, NY) driven by a stepper motor. After leaving the delay line, the probe laser beam joins the pump beam at a flint glass, beam-combining prism (Melles Griot, Irvine, CA). The angle between the two dye laser beams at the prism is adjusted so that the two beams emerge collinearly.

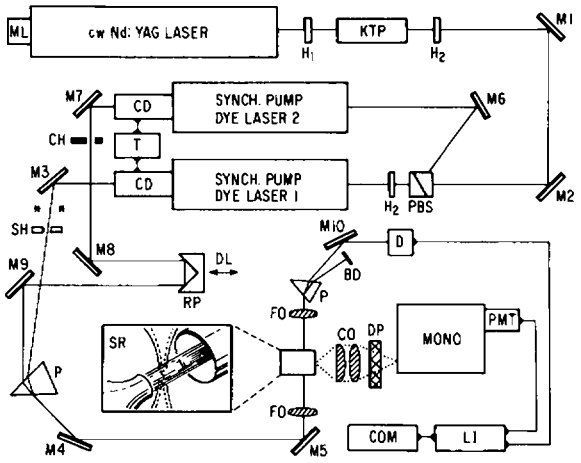

FIGURE 1 Instrumentation designed to sequentially record picosecond time-resolved fluorescence (PTRF) and picosecond transient absorption (PTA) data using the same experimental conditions. L, mode-locker; H1, half wave plate (1,064 nm); H2, half wave plate (532 nm); M1-M10, front surface dielectrically coated mirrors; PBS, polarizing beam splitter; CD, cavity dumper; T, timing synchronization; CH, position of the mechanical chopper for PTRF measurements; **, position of the mechanical chopper for PTA measurements; SH, mechanical shutter used with pump laser beam; DL, optical delay line; RP, retroprism; P, prism used either for combining or dispersing pump and probe beams; FO, optics used for either focusing or collimating the pump and probe beams; SR, sample region showing collinear laser beams and flowing liquid jet of BR; D, sensitive photodiode; BD, beam dump; CO, collecting optics for fluorescence; DP, depolarizer; MONO, monochromator; PMT, photomultiplier tube; LI, lock-in amplifier; COM, computer.

An autocorrelator (model CR-290; Coherent Inc.) is used to measure the pulse duration of the pump and the probe laser beams. The autocorrelator also is used to measure the cross-correlation between the two collinear dye laser beams. Cross-correlation measurements permit the two pulses to be brought into temporal coincidence with a precision of ±1.5 ps. Power measurements are made with a calibrated photovoltaic device (model 212; Coherent Inc.). All the pulse durations reported in this paper are real-time values obtained by converting the corresponding autocorrelation or cross-correlation measurements.

The aqueous suspension of PM is pumped from a chilled reservoir (10°C) through a 380-μm (ID) glass nozzle in a direction horizontal to the laser table (i.e., perpendicular to the plane defined by the vertical entrance slit of the monochromator and the vertical axis of the two laser beams). The collinear dye laser beams are focused to a 18-μm diam spot in the flowing sample by an achromatic microscope objective (Leitz NPL 5X). This 18-μm spot has been measured with the knife edge method (49) assuming a Gaussian profile. The BR sample leaves the nozzle with a velocity of 20 m/s. This velocity is sufficient to ensure that the sample volume defined by the 18-μm laser spot size is completely removed from the path of the pump and probe laser beams during the one microsecond between successive pairs of laser pulses (i.e., both the pump and probe dye lasers operate at a 1-MHz repetition rate). This flow rate and focusing volume ensure that each pair of pump and probe pulses intersects a fresh volume of sample.

For the PTRF measurements, the emission from the sample is collected by a spherical optic aligned so that its optical axis is perpendicular to the plane formed by the two laser beams and the flowing liquid sample. The collecting optic consists of an F/1, two lens condenser (model 01CMP123; Melles Griot) made of synthetic fused silica. The fluorescence is focused onto the entrance slit of an F/9, one meter, Czerny-Turner scanning spectrometer (model 1704; Spex Industries, Inc., Edison, NJ) with a 1,200 line/mm, conventionally ruled grating operating in the first order of diffraction. The dispersed signal is detected by a high gain photomultiplier (PMT) (model R-943/02; Hamamatsu Corp., Middlesex, NJ) attached to the exit slit of the spectrometer. The gallium arsenide photocathode of this PMT provides good sensitivity in the near infrared. The PMT is cooled thermoelectrically to −30°C to reduce electronic noise. The width of the entrance and exit slits is maintained at 1 mm, to provide a spectral bandwidth of 0.7 nm. The intense Rayleigh scattering from the sample is greatly attenuated by a low pass, color filter (No. 2-60; Corning Science Products, Corning, NY) placed in front of the entrance slit of the spectrometer. The PMT signal is processed by a lock-in amplifier (Ortec Brookdeal model 3505SC). A mechanical chopper is inserted in the path of the probe laser beam (position CH in Fig. 1) to produce a chopping frequency (500 Hz) needed as a reference for the lock-in amplifier. Since only the probe laser beam is chopped at 500 Hz, it is feasible to monitor only the fluorescence signal induced by the probe laser beam at a given time delay after excitation. The signal from the lock-in amplifier is digitalized and stored in a microcomputer.

For the PTA measurements, both pump and probe laser beams are passed through a second microscope objective (Leitz NPL 5X) for recollimation. The beams are spatially separated by a dispersive prism. The pump beam is blocked while the probe beam is directed to a slow response, high sensitivity photodiode (model HUV-2000B; EG&G Photon Devices). The signal from the photodiode is sent to the input of the lock-in amplifier which is triggered at the frequency of a chopper placed in the path of the pump laser only (at position ** in Fig. 1).

C. Procedures

Two types of experimental procedures are followed to obtain the fluorescence results reported here. The first procedure determines the experimental conditions appropriate for exciting fluorescence during the time-resolved experiment. It involves one dye laser (i.e., dye laser 2 in Fig. 1) operating at 590 nm to both initiate the photocycle and to excite fluorescence. By varying the pulse energy of this single laser, the laser-energy threshold below which no significant photochemistry occurs can be determined. The second procedure is designed to obtain time-resolved fluorescence data. This procedure uses two picosecond dye lasers in a pump and probe configuration (Fig. 1). One dye laser (laser 1 in Fig. 1) operating at 565 nm initiates the BR photocycle, whereas the second dye laser (laser 2 in Fig. 1) operating at 590 nm excites the fluorescence from any species present at a given time delay after the photocycle begins. In order to obtain time-resolved fluorescence spectra, the time delay between the pump and probe laser pulses is fixed and the fluorescence spectrum initiated by the probe laser is recorded by scanning the spectrometer under computer control over the spectral region from 650 to 880 nm.

To measure the relative change of absorbance in the BR sample induced by the pump beam, the PTA procedure is composed of two steps. First, the pump beam is chopped at a given frequency, ω, and the variation of the transmitted probe beam is detected by phase-sensitive methods locked to ω. These data provide a measurement of ΔI (50). Second, the probe beam is chopped in order to detect the intensity of the laser transmitted through the sample, I, while the pump beam is blocked from reaching the sample. The change of absorbance, ΔA, is then obtained by

$$\Delta A = -\Delta I/[(I) \ln (10)].$$

D. Data treatment

Fluorescence spectra are recorded over the 650–880-nm range in 2-nm spectral intervals before being digitalized and are smoothed using a least-squares fit function over 17 points (51). The fluorescence spectrum is obtained by averaging the signal from 10^6 pairs of pump-probe laser pulses. The signal-to-noise ratio (S/N) of the resultant fluorescence is 10^3. Because these spectra extended over a wide spectral range, they are corrected for the spectral transmission of the detection system which includes the collecting optic, filter, diffraction grating, and the PMT. For this correction, the polarization of the emission and polarization dependence of the grating must be considered. The insertion of a depolarizer between the collecting optic and the entrance slit addresses these questions by randomizing the polarization seen by the spectrometer. Thus, with this depolarizer in place, the response of the entire detection system is the same for all polarizations of the emission.

The spectral transmission curve of the detection system is determined according to published procedures (52, 53). This curve is measured using a 10-W quartz halogen-iodine, tungsten filament lamp (Oriel No. 6318) which is voltage stabilized at 6 DC volts to provide a constant color temperature of 3,150 K. The spectral emission of this lamp has been well characterized (54) and is used to obtain a standard spectral source for calibration. Care has been taken to ensure that the experimental conditions used for spectral calibration closely mimic those used to collect emission from the BR photocycle. For example, a magnesium oxide diffuser, the reflectivity of which is constant from 650 to 880 nm (55), is inserted in the same spatial position normally occupied by the sample in order to reflect emission from the calibration lamp into the spectrometer. The spectrometer is scanned to record the spectrum over the spectral range of interest. When this spectrum is divided by the emissivity of the lamp, a spectral transmission curve which can be used to correct all the fluorescence spectra is obtained.

The reabsorption of the emission by the 380-μm pathlength within the sample jet is not considered in the calibration procedure since it makes a negligible contribution to intensity changes.

RESULTS

The high degree to which BR-570 is optically coupled to the initial photocycle intermediates such as J-625 and K-590 is illustrated by their strongly overlapping absorption spectra (24). Excitation of BR-570 used to initiate the photocycle also can be absorbed by both J-625 and K-590. As a consequence, both fluorescence and photochemistry involving J-625 and K-590 can occur if a significant concentration of either intermediate is formed during the excitation process. In general, the optical conditions used for pumping the photocycle and for optically probing are of utmost importance since they control not only the fluorescence signals measured, but also the photochemical formation of the intermediates. The PTRF experiments described here are designed to hold the pumping conditions (wavelength, pulse duration, pulse energy) constant while the photocycle is monitored as a function of reaction time by an optical pulse which induces fluorescence from the reaction mixture, but remains itself photochemically nonperturbing. The versatility with which the pumping and probing conditions can be quantitatively controlled in these PTRF experiments is a departure from previously reported studies which makes it feasible to observe fluorescence from photocycle intermediates not previously reported.

The identification of emission assignable to a photocycle intermediate depends directly on a quantitative understanding of the fluorescence spectrum assignable to BR-570 and of the optical conditions for probing the photocycle by PTRF which remain photochemically nonperturbing. A probe laser wavelength of 590 nm is used at the outset since BR-570, J-625, and K-590 all absorb at this wavelength. Single laser experiments using 590 nm, therefore, provide both types of information simultaneously if emission is measured as a function of laser power (pulse duration fixed). These data identify the experimental conditions under which (*a*) fluorescence from BR-570 only can be generated and (*b*) no significant amount of photochemistry is initiated by the probe pulse.

The dependence of the fluorescence in the 650–880-nm region on the 590-nm laser power used to excite the BR sample is addressed by the data in Fig. 2 *A*. This dependence is manifested by changes in the spectral shape of the fluorescence as the laser power is increased from 2.4 to 38 mW (8-ps pulse duration and 1-MHz repetition rate). These two spectra have been scaled to have the same maximum value in order to facilitate a comparison of their respective shapes. As the laser power increases, a

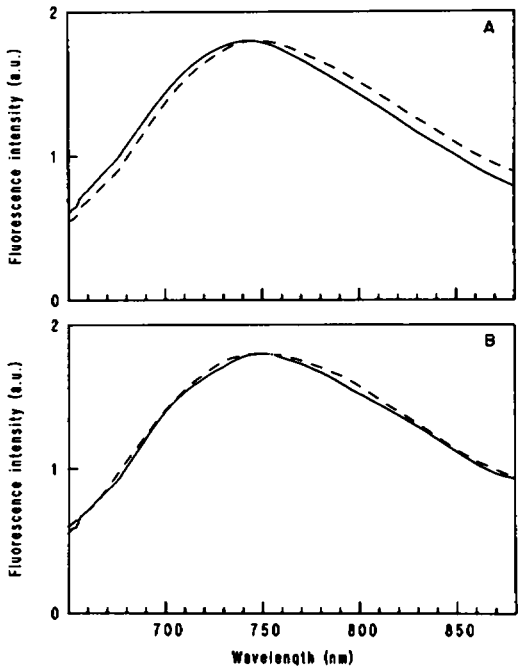

FIGURE 2 Fluorescence spectra of BR-570 at room temperature induced by a single, pulsed laser operating at 590 nm. (*A*) Fluorescence spectra obtained with 8-ps (FWHM) pulsewidth at 1-MHz repetition rate. Data presented as dashed line is recorded with peak power of 300 W (average power of 2.4 mW). Data presented as solid line is recorded with a peak power of 4.7 kW (average power of 38 mW). The intensity of these spectra are scaled to a common value at 748 nm to facilitate the comparison of their spectral shapes. When average powers exceed 6 mW, changes in shape of the fluorescence spectra appear that indicate the presence of photochemistry. By contrast, the spectra obtained with low average power excitation below 6 mW (*dashed line*) remain unchanged and, therefore, can be assigned to BR-570. (*B*) Fluorescence spectra obtained with 4-ps (FWHM) pulsewidth and with a peak power of either 8 W (*solid line*) or 600 W (*dashed line*). The repetition rates of the laser are 76 MHz (*solid line*) and 1 MHz (*dashed line*) providing an average power in both cases of 2.4 mW. The close similarity between the two fluorescence spectra obtained with peak power ranging over two orders of magnitude makes it feasible (*i*) to assign the low power fluorescence spectrum (*dashed line*) to BR-570 alone and (*ii*) to establish that the probe laser conditions used in PTRF and PTA experiments (i.e., 600 W) do not induce significant amounts of photochemistry.

relatively larger amount of fluorescence appears in the 650–730-nm region while a relatively smaller amount of fluorescence is observed in the 750–880-nm region. These changes in relative intensities reflect a change in the shape of the total fluorescence signal. Although the differences seen in Fig. 2 *A* are small, these fluorescence spectra are highly reproducible and consequently, the differences are meaningful. No significant changes occur until the laser power exceeds 6 mW and, in fact, the 6.5-mW spectrum is indistinguishable from that recorded with 2.4 mW. Based on these fluorescence results, excitations at powers below 6 mW do not produce significant photochemistry from BR-570 during the 8-ps pulse duration and, as a consequence, these low power fluorescence spectra can be assigned to BR-570 only. To our knowledge, these are the first fluorescence spectra of BR-570 reported using picosecond pulsed laser excitation.

A completely separate determination of the BR-570 fluorescence spectrum is obtained by using lower energy (31 pJ/pulse) 590-nm laser pulses at higher repetition rates. The fluorescence recorded with 2.4 mW (4-ps pulse duration) of 590-nm radiation delivered to the BR sample at a 76-MHz repetition rate is presented in Fig. 2 *B*. The comparable fluorescence spectrum obtained with 2.4 mW (4-ps pulse duration) at a 1-MHz repetition rate also is shown in Fig. 2 *B*. The peak powers of the laser excitation used in these two experiments differ by almost 10^2 (8 W versus 600 W) although the corresponding differences in repetition rates maintain the same average laser power and a comparable S/N value. No significant differences can be seen when these two low power spectra are compared to each other (Fig. 2 *B*) or when either is compared with the 2.4 mW (8-ps pulse duration) shown in Fig. 2 *A*. When the laser power is below 6 mW, there is no evidence from any of these fluorescence data to indicate substantial photochemistry from BR-570 even though the pulse duration (4–8 ps) and the repetition rate (1–76 MHz) for excitation have changed. All of the corresponding fluorescence spectra are assigned to BR-570 only.

In selecting the experimental parameters most appropriate for a probe laser in a PTRF experiment, the relationship between pulse repetition rate and the rate at which the BR liquid sample can be exchanged through the irradiated volume must be considered. With a pulse repetition rate of 76 MHz, a sample flow rate of 20 m/s and an irradiated volume of 18 μm, each BR sample volume is excited repeatedly (76 times) by separate laser pulses. The secondary chemistry which might be initiated by such repetitive excitation from intermediates can be avoided if the pulse repetition rate is lowered to 1 MHz since the sample volume is completely exchanged within the 18-μm irradiated volume every 0.9 μs. There is minimal optical perturbation of the BR photocycle by the probe laser if it is operated at 1-MHz repetition rate and with a power of 6 mW or less. Thus, a probe laser operated with 2.4-mW average powers (4-ps pulse duration) at 1-MHz repetition rates is photochemically nonperturbing with respect to BR-570 for this sample arrangement. It is assumed that both J-625 and K-590 have photochemical thresholds similar to that for BR-570. These are the experimental parameters used in the PTRF results described here.

PTRF spectra are presented in Fig. 3 for time delays between 0 and 40 ps. The fluorescence spectrum of

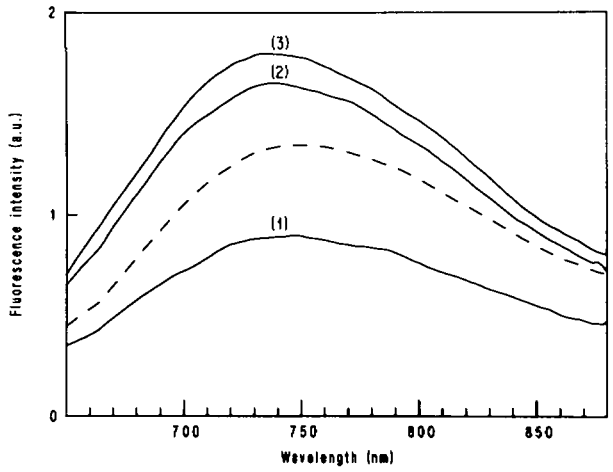

FIGURE 3 PTRF spectra obtained with an 8-ps (FWHM) pump laser pulse at 565 nm (17.5 mW) and a 4 ps (FWHM) probe laser pulse at 590 nm (2.4 mW) occurring at (*1*) 0-ps delay (i.e., cross-correlation time), (*2*) 20-ps delay, and (*3*) 40-ps delay. Both pump and probe lasers are operated at 1-MHz repetition rates. The dashed line represents the fluorescence spectrum of BR-570 alone excited only with the 590-nm probe laser pulses (same spectrum shown in Fig. 2 *B*, *dashed line*). The increase of fluorescence above the level assignable to BR-570 alone (i.e., probe laser only level) appearing for delays of 20 and 40 ps indicates that a transient species in the BR photocycle fluoresces with a quantum efficiency that exceeds that of BR-570.

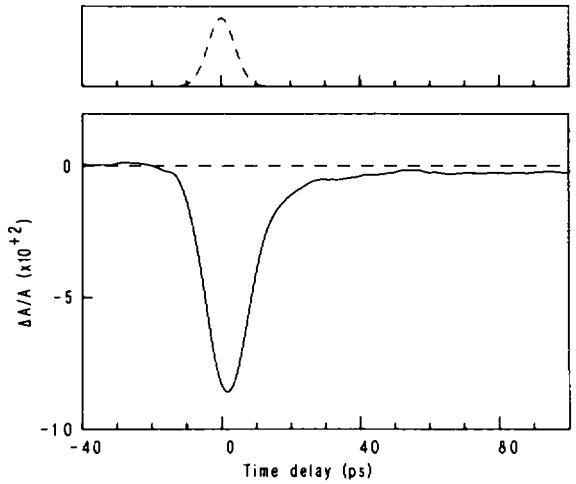

FIGURE 4 The change in relative absorbance ($\Delta A/A$) at 590 nm induced by an 8-ps (FWHM) laser pulse at 565 nm as a function of delay time for a room temperature sample of BR. The cross-correlation function measured for the pump (8 ps) and probe (4 ps) laser pulses is shown as dashed lines in the top panel.

BR-570 (Fig. 2 *B*) is shown to facilitate comparison. All these spectra have been corrected for the spectral response of the detection system. For a 17.5-mW pump power (2.2-kW peak power), the 0-ps delay spectrum is ~30% lower in intensity than the BR-570 spectrum. This decrease reflects the smaller population of BR-570 during the pumping process. The 0-ps delay corresponds to the temporal overlap of the pump and probe pulses which is represented by the cross-correlation signal (shown schematically in the insert of Fig. 4). The pump pulse creates a mixture of species comprised of electronically excited BR-570 (BR*) as well as photochemical intermediate(s) formed within the duration of the pump pulse (i.e., 8 ps). The probe beam can generate fluorescence from all of the transient species except BR*, which absorbs at wavelengths less than 500 nm (24) and does not absorb significantly at 590 nm. Fluorescence from the ground-state BR-570 remaining in the mixture, of course, contributes to the measured signal. The fluorescence spectra recorded at time delays of 20 ps and longer are larger in intensity than the BR-570 spectrum. This increased intensity signals the presence of fluorescence from species other than BR-570.

These results can be viewed with respect to those expected if BR-570 is the only photocycle species to emit. If the only phenomenon under observation is the optical excitation of BR-570 followed by the photophysical relaxation of BR*, then the fluorescence signal could reach only the level produced by the probe laser (measuring the original concentration of BR-570). Correspondingly, if BR* undergoes photochemical decay to intermediates such as J-625 and K-590 and if neither of these fluoresce (as concluded in the literature [39, 41–46]), then the intensity of the fluorescence spectrum could only reach a level below that measured with the probe laser only. By contrast with these expectations, however, PTRF spectra in Fig. 3 (20 and 40 ps) have intensities which exceed that of the probe laser only by more than 40%. In addition, the PTRF spectra for time delays ranging from 20 to 100 ps exhibit a distinctly different shape than that obtained with the probe laser only (Fig. 3). The changing shape of the fluorescence spectrum in PTRF measurements is similar to that observed for increasing laser power in the single laser results (Fig. 2 *A*).

The time evolution of the relative change of absorbance, $\Delta A/A$, can be monitored directly by observing the PTA signal as the optical delay line is scanned. PTRF and PTA data are recorded sequentially on the same BR sample and, therefore, can be directly compared. The 590-nm PTA data measured over the initial 100 ps (Fig. 4) are in good agreement with those reported in the literature (24).

DISCUSSION

The fluorescence spectroscopy of the BR photocycle has been examined in at least eight previous studies on either

room temperature, liquid samples (39–42), or on low (77 K) temperature film samples (43–46). Direct comparisons of these data are difficult not only because of the differences in sample media and temperatures, but also because the optical excitation conditions varied widely. The high degree to which the initial (i.e., picosecond) intermediates are photolytically coupled to one another suggests that significantly different molecular mixtures are prepared when excitation conditions are changed and that a direct comparison of emission data from these various studies may not be warranted. The substantial differences between the fluorescence data currently available (both in the literature and presented here) therefore, may be attributed primarily to these variations in excitation conditions. This point can be illustrated well by the various fluorescence spectra reported above for BR-570. It also is important to note that with the exception of one group, all previous workers have concluded that the emission observed from the BR photocycle is assignable to BR-570 alone. This common conclusion has been reached in spite of clear variations in the experimental data on which it is based. The studies which stand as exceptions (21, 43, 46) have assigned emission shifted to the red from that of BR-570 to an intermediate identified as P-BR which is explicitly distinguished from either J-625 or K-590. Thus, no previous study has assigned any emission to K-590 and, in fact, many have specifically excluded it from such an assignment. In reviewing the literature, special attention is given here to identifying the excitation conditions used in each study in order to understand how the emission observed could have been assigned exclusively to BR-570 and not to a photocycle intermediate. For comparative purposes, attention also is given to the experimental approach used in this work which is designed specifically to resolve emission from a picosecond intermediate.

The fluorescence spectrum of BR-570 in room temperature solution has been reported in several studies, the earliest of which was Lewis and co-workers (41). Continuous laser excitation at 514.5 nm was used to obtain broad, unstructured emission extending from the visible to the near infrared with a maximum near 790 nm. Subsequent investigations using cw laser excitation also recorded unstructured emission spectra with intensity maxima ranging from 700 nm (45) and 714 nm (46) with 580-nm excitation to 660 nm (44) with 530-nm excitation. The differences in the emission maxima reported in these early studies are attributable to differences in the excitation conditions and the sample preparations used. For example, these measurements utilized cw excitation sources operating at a variety of wavelengths and intensities and examined static BR samples with volumes ranging from microliters contained in a capillary tube to a few milliliters in an unstirred cuvette. In addition, a variety of sample concentrations and suspension media were used. It is reasonable to conclude that since the excitation conditions were different, the photolytically generated mixture of BR photocycle species from which emission was collected also varied from one study to the next. It is therefore not surprising that these emission spectra exhibit significantly different spectral profiles and intensity maxima and that the fluorescence spectrum reported here (Fig. 2 *B*) is not in good agreement with any of these early results. Although the principal reason for this disagreement is probably associated with the excitation conditions, it also should be noted that there are significant differences in the sample preparation, purification procedures, and methods of spectral correction in the treatment of the extremely weak emission of room temperature liquid samples.

More recent fluorescence studies have addressed the photolytic conversion occurring during the early stages of the photocycle by using extremely low intensity excitation designed to minimize photolysis and thereby to obtain emission from BR-570 alone. Low intensity excitation at 546 nm (from a high pressure Hg lamp [42]) and at 514.5 nm (from a cw laser [24]) has been used to obtain very similar BR-570 fluorescence spectra as is shown schematically in Fig. 5. In the second of these studies (24), the intensity of the cw laser excitation was increased by an order of magnitude without changing the fluorescence spectrum in order to demonstrate that no significant amount of photochemistry had occurred. As discussed above, the same type of experimental approach is used in this work except that picosecond, pulsed excitation is used to record a BR-570 fluorescence spectrum which is in

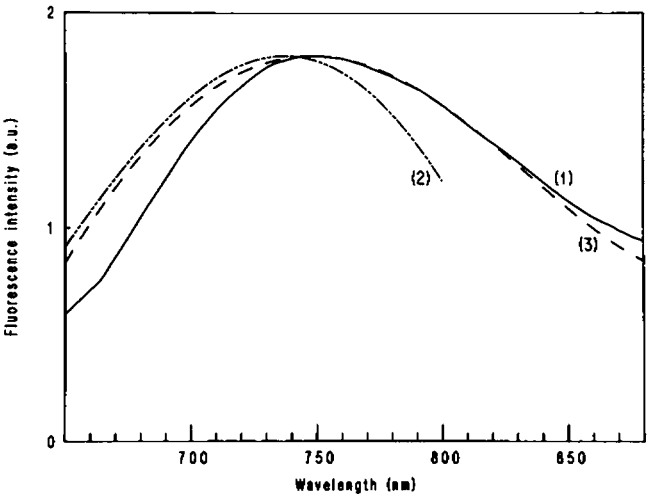

FIGURE 5 Comparison of the fluorescence spectrum assigned to BR-570 reported in this paper (*1*) with recently published work by Poland et al. (*2*) (reference 24) and by Kouyama et al. (*3*) (reference 42).

good agreement with those obtained with low power, cw laser excitation (Fig. 5). The small differences observed in the 650–700-nm region of Fig. 5 can be attributed to differences in the excitation wavelength and the accumulated errors arising from spectral corrections (e.g., the wavelength-dependent response of gratings and detectors). The somewhat lower intensity of the spectrum between 750 and 800 nm reported by Polland et al. (24) may be caused by the decreasing sensitivity of that detector near 800 nm.

The BR-570 emission spectrum also has been obtained from 77-K films. In fact, most emission studies have been performed on such samples since it is thought that the photocycle does not function at 77 K, but rather that only K-625 is formed (47). In principle, therefore, time-resolved measurements are not required to observe emission from an intermediate. Unlike the room temperature results, the emission spectrum at 77 K is structured with distinct maxima at 678, 733, and 791 nm (41). All of the studies report structured emission although the positions of intensity maxima vary (39). If only BR-570 and K-625 are present at 77 K in samples that are preilluminated with visible radiation (47), then fluorescence assignable to these species should be detectable. In two such preillumination studies (40, 41), a decrease in emission intensity was observed which was interpreted in terms of the conversion of BR-570 to K-625. All of the detected emission was assigned to BR-570. In three other studies using preillumination (43, 44, 46), a large increase in emission intensity characterized by a maximum shifted to the red (relative to the maximum of the BR-570 emission spectrum) was observed and attributed to a new intermediate, P-BR (specifically identified as distinct from K-625). Although these inconsistencies remain unresolved, the 77 K data are relevant to the room temperature results presented here with respect to three points: (*a*) the fluorescence spectrum of BR-570 is temperature dependent, exhibiting structure at 77 K, but no significant spectral shift in its intensity maximum as a function of temperature; (*b*) no emission has been assigned to K-625 even though the photocycle is thought not to function at 77 K; and (*c*) the emission properties associated with the P-BR intermediate are different from those assigned to K-590 in this work. Specifically, the intensity maximum of emission for P-BR is reported to appear to the red of the BR-570 fluorescence maximum while that for K-590 occurs to the blue.

In the room temperature results reported here, the presence of K-590 fluorescence is most evident in PTRF data taken with a delay time of 40 ps. Assuming, for simplicity, a linear reaction path for the early events in the photocycle:

$$\text{BR-570} \xrightleftharpoons{h\nu} \text{BR*} \rightarrow \text{J-625} \rightarrow \text{K-590},$$

the relative concentrations of each species at a given time, t, is given by

$$[\text{BR-570}]_i = [\text{BR-570}]_t + [\text{BR*-570}]_t + [\text{J-625}]_t + [\text{K-590}]_t,$$

where $[\text{BR-570}]_i$ is the initial concentration of BR. PTA results have shown that after 40 ps, K-590 is the only intermediate present (23, 24). The PTA data in Fig. 4 illustrate this point. At 40 ps, the 590-nm PTA signal closely approaches the absorbance of BR-590. Since 590 nm lies very near the isobestic point for the absorption spectra of BR-570 and K-590, these PTA data simply reflect the partial conversion of BR-570 into K-590. The PTRF spectrum at a 40-ps delay time (Fig. 3), therefore, is composed of contributions exclusively from BR-570 and K-590. Analogously, the large increase in fluorescence observed at 40 ps can be attributed to the formation of K-590. This conclusion is supported by considering two limiting cases: (*a*) if no photochemistry occurs upon excitation of BR-570 (i.e., BR* relaxes completely to BR-570), then the intensity of the PTRF spectrum at any time, t, could not exceed that of the probe laser only signal (dashed spectrum in Fig. 3), and (*b*) if photochemistry occurs upon excitation of BR-570, but no photocycle intermediate emits, then the PTRF spectrum intensity cannot reach that of the probe laser only signal ($[\text{BR-570}]_t < [\text{BR-570}]_i$ because of photochemistry). The detection of fluorescence above the $[\text{BR-570}]_i$ level demonstrates that at least one photocycle intermediate emits while the fact that the increased fluorescence reaches a maximum at a 40-ps delay (and then remains constant) requires its assignment to K-590.

The fluorescence spectrum at K-590 can be obtained from the PTRF data if a value for the photochemical quantum efficiency, PQE, is determined. The PQE is defined in terms of a specific photocycle intermediate at a particular time. For the case of K-590 fluorescence at 40 ps, PQE is defined as $[\text{K-590}]_{40\text{ ps}}/[\text{BR-570}]_i$. The PQE is directly dependent on the quantum yield (QY) associated with BR* (i.e., QY is given by the relative amount of J-625 formed from BR*). Previous workers have reported QY values ranging from 0.3 (16) to 0.6 (56). A rate equation model simulating the relative concentration of primary photocycle intermediates explicitly determines the functional dependence of PQE on each value of QY. The parameters for this simulation are derived from fits to transient absorption and fluorescence data measured over the initial 100-ps interval of the BR photocycle. For QY ranging from 0.3 to 0.6, a PQE of ~0.4 is obtained from such simulations (Atkinson et al., manuscript in preparation). The K-590 fluorescence spectrum at a 40-ps delay, based on a PQE value of 0.4, is presented in Fig. 6. This spectrum, which can be readily distinguished from the BR-570 fluorescence spectrum, does not change for

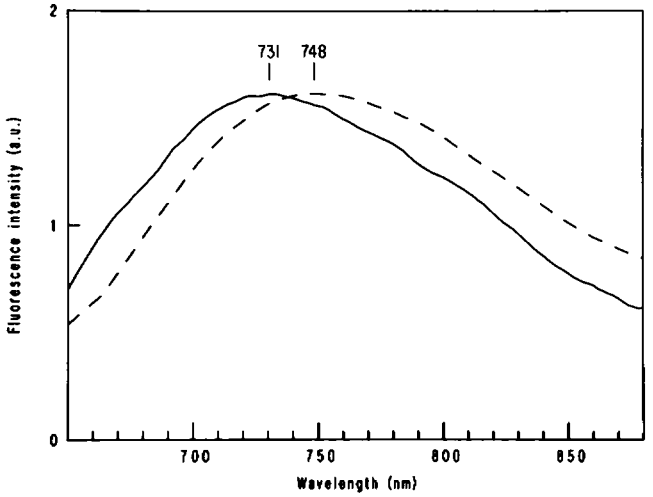

FIGURE 6 Fluorescence spectrum of the K-590 intermediate in the BR photocycle obtained at room temperature and with 590-nm probe excitation. The fluorescence spectrum of BR-570 at room temperature recorded with pulsed (2.4 mW) excitation at 590 nm is shown as a dashed line (also see Fig. 2) for comparison. The K-590 spectrum is obtained by subtracting the scaled (0.6) BR-570 fluorescence spectrum from the 40-ps PTRF spectrum (Fig. 3). This analysis is based on the conclusion that, 40% of the initial concentration of BR-570 is converted into K-590. See text for discussion.

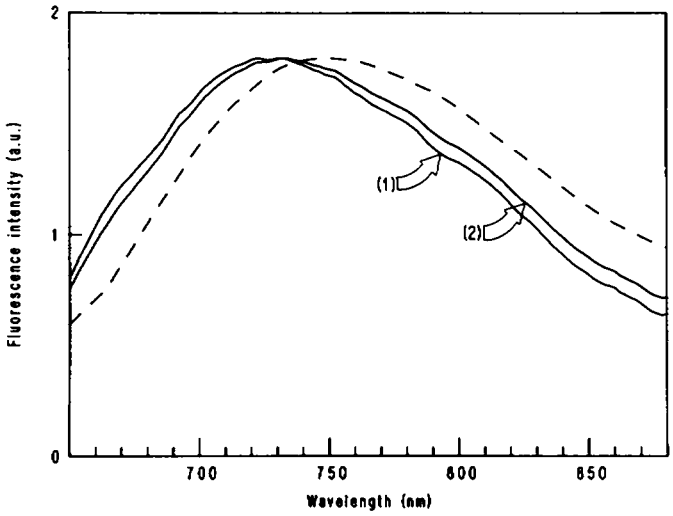

FIGURE 7 Fluorescence spectra potentially assignable to the K-590 intermediate derived from an analysis using two different photochemical quantum efficiencies (PQE) for the conversion of BR-570 into K-590: (*1*) 30%, and (*2*) 50%. These fluorescence spectra are obtained by subtracting different scaled (0.7 or 0.5, respectively) BR-570 fluorescence spectra from the PTRF spectrum recorded at a 40-ps delay. The fluorescence spectrum of BR-570 at room temperature recorded with pulsed (2.4 mW) excitation at 590 nm is shown as a dashed line (also see Fig. 2) for comparison. Each of these three fluorescence spectra can be readily distinguished from that assigned to BR-570. See text for discussion.

time delays at least as long as 100 ps, a period over which PTA results (Fig. 4) also have shown the K-590 concentration to be constant (also see reference 24).

Although a specific PQE value is required to obtain the precise K-590 fluorescence spectrum from an analysis of PTRF data, the general characteristics of the K-590 fluorescence spectrum are not altered greatly if the PQE ranges from 0.3 to 0.5. This point is illustrated in Fig. 7 where the BR-570 fluorescence spectrum (Fig. 2 *B*), after being multiplied by factors of 0.3 or 0.5, has been substracted from the 40-ps PTRF spectrum (Fig. 3). The maximum intensities of the resultant difference spectra have been scaled to a common value and plotted together with the fluorescence spectrum of BR-570 for the purpose of comparison. Although both the intensity maximum and the shape are affected somewhat by the value of the PQE chosen, the fluorescence attributable to K-590 can be readily distinguished from that of BR-570 in all cases. The general identification and characterization of the PTRF spectrum of K-590, therefore, does not depend critically on where the PQE value lies between 0.3 and 0.5.

The 17-nm blue shift between the fluorescence maxima of BR-570 and K-590 is clearly seen in Fig. 6. When viewed in relation to their respective absorption spectra, K-590 is found to have a significantly smaller Stokes shift than BR-570 (141 nm versus 178 nm). Such a reduced Stokes shift reflects a smaller change in geometry between the ground and excited electronic states of K-590 than for the corresponding states of BR-570. This difference also is reflected in the larger fluorescence quantum yield observed for K-590 (ϕ_f^K). The value of ϕ_f^K can be calculated from the PTRF data shown in Fig. 3 by assuming the entire 40% increase of fluorescence signal is due to K-590. Since the absolute value of ϕ_f^{BR} has been reported to be 10^{-4} (41), the value of ϕ_f^K is 2×10^{-4}.

Results from two other studies (57, 58) are consistent with the observations reported here. Specifically, the reduced Stokes shift and larger fluorescence yield for K-590 may reflect the storage of energy in K-590 (~15 kcal/mol) resulting from the primary photocycle events (57). These observations also are consistent with model calculations which utilize the C_{13}=C_{14} torsion as the major reaction coordinate underlying the primary photochemistry (58). These calculations conclude that the excited-state relaxation away from the Franck-Condon states initially populated in absorption is slower in K* than in BR*, thus suggesting that fluorescence from K* should appear to the blue of fluorescence from BR*.

Finally, the room temperature observations reported here should be considered in relation to those obtained at low (77 K) temperatures (43–46) where experiments are

designed to thermally trap the K intermediate. It has been reported that the K intermediate formed at 77 K (K-625) does not fluoresce (43–46). Since the PTRF techniques described here have not yet been applied to 77-K samples, no direct comparisons with room temperature results can be made. It remains uncertain, therefore, whether the differences in fluorescence measurements arise from (*a*) differences in the fluorescence properties of low temperature K versus K-590, (*b*) the degree of success in thermally trapping the K-intermediate, or (*c*) the capability of the different laser techniques utilized to distinguish fluorescence from the K-intermediate.

Mechanism for primary processes

The PTRF data presented in this paper provide new information to be incorporated into the molecular mechanism used to describe the primary processes in the BR photocycle.

(*a*) The detection of fluorescence from K-590 characterizes the excited electronic state of a photocycle intermediate for the first time. Both the smaller Stokes shift and increased fluorescence quantum yield not only distinguish the electronic transitions of K-590 from that in BR-570, but also suggest that a significantly different change in molecular geometry occurs in the two species upon optical excitation.

(*b*) Low (77 K) temperature data should be reevaluated in terms of emission assignable to K-590.

(*c*) The appearance of a fluorescence spectrum which remains unchanged in shape and spectral position over the initial 100 ps of the photocycle is the basis of an excellent spectral signature for K-590 that can be utilized to measure its kinetic behavior.

The technical assistance of workers in the Department of Biochemistry at the University of Arizona in the preparation of bacteriorhodopsin is gratefully acknowledged. The authors also gratefully acknowledge James B. Day for the sample preparations.

This research was supported by a grant from the National Institutes of Health. Cells of *H. halobium* were kindly supplied by Professor W. Stoeckenius, Department of Biochemistry and Biophysics, University of California at San Francisco.

Received for publication 15 February 1988 and in final form 3 October 1988.

REFERENCES

1. Oesterhelt, D., and W. Stoeckenius. 1971. Rhodopsin-like protein from the membrane of *Halobacterium halobium*. *Nature New Biol.* 233:149–152.
2. Oesterhelt, D., and W. Stoeckenius. 1973. Functions of a new photoreceptor membrane. *Proc. Natl. Acad. Sci. USA.* 70:2853–2857.
3. Oesterhelt, D. 1976. Bacteriorhodopsin as an example of a light-driven proton pump. *Angew. Chem. Int. Ed. Engl.* 15:17–24.
4. Stoeckenius, W. 1980. Purple membrane of halobacteria: a new light-energy converter. *Acc. Chem. Res.* 13:337–344.
5. Unwin, P. N. T., and R. Henderson. 1974. Molecular structure determination by electron microscopy of unstained crystalline specimens. *J. Mol. Biol.* 94:425–440.
6. Henderson, P., and P. N. T. Unwin. 1975. Three-dimensional model of purple membrane obtained by electron microscopy. *Nature (Lond.).* 257:28–32.
7. Khorana, H. G., G. E. Gerber, W. C. Heilihy, C. P. Gray, R. J. Anderegg, K. Nikei, and K. Biemann. 1979. Amino acid sequence of bacteriorhodopsin. *Proc. Natl. Acad. Sci. USA.* 76:5046–5050.
8. Ovchinnikov, Yu. A., N. G. Abdulaev, M. Yu Feigina, A. V. Kiselev, and N. A. Lobanov. 1979. The structural basis of the functioning of bacteriorhodopsin: an overview. *FEBS (Fed. Eur. Biochem. Soc.) Lett.* 100:219–224.
9. Stoeckenius, W., and R. A. Bogomolni. 1982. Bacteriorhodopsin and related pigments of halobacteria. *Annu. Rev. Biochem.* 51:587–616.
10. Marcus, M. A., and A. Lewis. 1977. Kinetic resonance Raman spectroscopy: dynamics of deprotonation of the Schiff base of bacteriorhodopsin. *Science (Wash. DC)* 195:1328–1330.
11. Hsieh, C. L., M. Najumo, M. Nicol, and M. A. El-Sayed. 1981. Picosecond and nanosecond resonance Raman studies of bacteriorhodopsin. Do configuration changes of retinal occur in picoseconds? *J. Phys. Chem.* 85:2714–2717.
12. Braiman, M., and R. Mathies. 1982. Resonance Raman spectra of bacteriorhodopsin's primary photoproduct: evidence for a distorted 13-cis retinal chromophore. *Proc. Natl. Acad. Sci. USA.* 79:403–407.
13. Cherry, R. J. 1982. Transient dichroism of bacteriorhodopsin. *Methods Enzymol.* 88:248–254.
14. Lozier, R. H., R. Bogomolni, and W. Stoeckenius. 1975. Bacteriorhodopsin: a light-driven proton pump in *Halobacterium halobium*. *Biophys. J.* 15:955–962.
15. Kaufmann, K. J., P. M. Rentzepis, W. Stoeckenius, and A. Lewis. 1976. Primary photochemical processes in bacteriorhodopsin. *Biochem. Biophys. Res. Commun.* 68:1109–1115.
16. Goldsmidt, C. R., M. Ottolenghi, and R. Korenstein. 1976. On the primary quantum yields in the bacteriorhodopsin photocycle. *Biophys. J.* 16:839–843.
17. Applebury, M. L., K. S. Peters, and P. M. Rentzepis. 1978. Primary intermediates in the photochemical cycle of bacteriorhodopsin. *Biophys. J.* 23:375–382.
18. Ippen, E. P., C. V. Shank, A. Lewis, and M. A. Marcus. 1978. Subpicosecond spectroscopy of bacteriorhodopsin. *Science (Wash. DC).* 200:1279–1281.
19. Dinur, U., B. Honig, and M. Ottolenghi. 1981. Analysis of primary photochemical processes in bacteriorhodopsin. *Photochem. Photobiol.* 33:523–527.
20. Shichida, Y., S. Matuoka, Y. Hidaka, and T. Yoshizawa. 1983. Absorption spectra of intermediates of bacteriorhodopsin measured by laser photolysis at room temperatures. *Biochim. Biophys. Acta.* 723:240–246.

21. Gilbro, T., and V. Sundstrom. 1983. Picosecond kinetics and a model for the primary events of bacteriorhodopsin. *Photochem. Photobiol.* 37:445–455.

22. Nuss, M. C., W. Zinth, W. Kaiser, E. Kolling, and D. Oesterhelt. 1985. Femtosecond spectroscopy of the first events of the photochemical cycle in bacteriorhodopsin. *Chem. Phys. Lett.* 117:1–7.

23. Sharkov, A. V., A. V. Pakulev, S. V. Chekalin, and Y. A. Matveetz. 1985. Primary events in bacteriorhodopsin probed by subpicosecond spectroscopy. *Biochim. Biophys. Acta.* 808:94–102.

24. Polland, H-J., M. A. Franz, W. Zinth, W. Kaiser, E. Kolling, and D. Oesterhelt. 1986. Early picosecond events in the photocycle of bacteriorhodopsin. *Biophys. J.* 49:651–662.

25. Atkinson, G. H. 1982. Time-resolved Raman spectroscopy. *In* Advances in Laser Spectroscopy. Vol. 1. B. A. Garetz and J. R. Lombard, eds. Heyden and Sons, Inc., New York. 155–175.

26. Atkinson, G. H. 1982. Time-resolved Raman spectroscopy. *In* Advances in Infrared and Raman Spectroscopy. Vol. 9. R. J. H. Clark and R. E. Hester, eds. North-Holland Publishers, London. 1–62.

27. Atkinson, G. H., and J. B. Pallix. 1983. Time-Resolved resonance Raman spectroscopy of excited triplet state all-trans retinal, excitation profiles, intersystems crossing kinetics, and O_2 quenching. *In* Photochemistry and Photobiology. Vol. 1. A. H. Zeweil, ed. Harwood Academic, New York. 705–716.

28. Atkinson, G. H., ed. 1983. Time-Resolved Vibrational Spectroscopy. Academic Press, Inc., New York. 398 pp.

29. Irwin, M. J., and G. H. Atkinson. 1981. Low-frequency resonance Raman spectroscopy of the deoxyhaemoglobin transient of photolysed carboxyhaemoglobin. *Nature (Lond.).* 293:317–318.

30. Atkinson, G. H. 1986. Molecular dynamics of liquid phase reactions by time-resolved resonance Raman spectroscopy. *In* Advances in Chemical Reaction Dynamics. P. Rentzepis and C. Capellos, eds. D. Reidel Publishing, Holland. 179–205.

31. Stockburger, M. and T. Alshuth, D. Oesterhelt, and W. Gärtner. 1986. Resonance Raman spectroscopy of bacteriorhodopsin: structure and function. *In* Advances in Infrared and Raman Spectroscopy. Vol. 13. R. J. H. Clark and R. E. Hester, eds. John Wiley & Sons, Inc., New York. 483–535.

32. Grieger, I., and G. H. Atkinson. 1984. Time-resolved resonance Raman spectroscopy of intermediates in the bacteriorhodopsin photocycle: direct photoconversion of BR-570 to M and M'. *In* Time-Resolved Laser Raman Spectroscopy. D. Phillips and G. H. Atkinson, eds. Harwood Academic, New York. 143–158.

33. Hsieh, C. L., M. A. El-Sayed, M. Nicol, M. Nagumo, and J-H. Lee. 1983. Time-Resolved resonance Raman spectroscopy of the bacteriorhodopsin photocycle on the picosecond and nanosecond time scales. *Photochem. Photobiol.* 38:83–94.

34. Stern, D., and R. Mathies. 1985. Picosecond and nanosecond resonance Raman evidence for structural relaxation in bacteriorhodopsin's primary photoproduct. *In* Time-Resolved Vibrational Spectroscopy. Vol. 4. A Laubereau and M. Stockburger, eds. Springer-Verlag, New York. 250–254.

35. Atkinson, G. H., I. Grieger, and G. Rumbles. 1985. Picosecond time-resolved resonance Raman spectroscopy of bacteriorhodopsin intermediates. *In* Time-Resolved Vibrational Spectroscopy. Vol. 4. A. Laubereau and M. Stockburger, eds. Springer-Verlag, New York. 255–258.

36. Atkinson, G. H., T. L. Brack, I. Grieger, G. Rumbles, D. Blanchard, and L. M. Siemankowski. 1985. Picosecond time-resolved resonance Raman vibrational spectroscopy. *In* Time-Resolved Vibrational Spectroscopy. G. H. Atkinson, ed. Gordon and Breach Science Publishers. 55–82.

37. Atkinson, G. H., T. L. Brack, D. Blanchard, G. Rumbles, and L. Siemankowski. 1986. Picosecond conformational intermediates in the bacteriorhodopsin photocycle. *In* Ultrafast Phenomena V. Vol. 46. G. R. Fleming and A. E. Siegman, eds. Springer-Verlag, Berlin. 46:409–412.

38. Atkinson, G. H. 1987. Picosecond intermediates in the bacteriorhodopsin photocycle. *In* Primary Processes in Photobiology. Vol. 20. T. Kobayashi, ed. Springer-Verlag, Berlin. 213–222.

39. Lewis, A., and G. J. Perreault. 1982. Emission spectroscopy of rhodopsin and bacteriorhodopsin. *Methods Enzymol.* 88:217–229.

40. Govindjee, R., and T. Ebrey. 1986. Light emission from bacteriorhodopsin and rhodopsin. *In* Light Emission by Plants and Bacteria. R. Govindjee, J. Amesz, and D. C. Fork, eds. Academic Press, Inc., New York. 401–419.

41. Lewis, A., J. P. Spoonhower, and G. J. Perreault. 1976. Observation of light emission from a rhodopsin. *Nature (Lond.).* 260:675–678.

42. Kouyama, T., K. Kinosita, Jr., and A. Ikegami. 1985. Excited state dynamics of bacteriorhodopsin. *Biophys. J.* 47:42–54.

43. Gillbro, T., N. Kriebel, and V. P. Wild. 1977. On the origin of the red emission of light adapted purple membrane of *Halobacterium halobium. FEBS (Fed. Eur. Biochem. Soc.) Lett.* 78:57–60.

44. Sineshchekov, V. A., and F. F. Litvin. 1977. Luminescence of bacteriorhodopsin from *Halobacterium halobium* and its connection with the photochemical conversions of the chromophore. *Biochim. Biophys. Acta.* 462:450–466.

45. Govindjee, R., B. Becker, and T. G. Ebrey. 1978. The fluorescence from the chromophore of the purple membrane protein. *Biophys. J.* 22:67–77.

46. Kriebel, A. N., T. Gillbro, and V. P. Wild. 1979. A low temperature investigation of the intermediates of the photocycle of light-adapted bacteriorhodopsin. *Biochim. Biophys. Acta.* 546:106–120.

47. Hurley, J. B., and T. G. Ebrey. 1978. Energy transfer in the purple membrane of *Halobacterium halobium. Biophys. J.* 22:49–66.

48. Oesterhelt, D., and W. Stoeckenius. 1974. Isolation of the cell membrane of *Halobacterium halobium* and its fractionation into red and purple membrane. *Methods Enzymol.* 31:667–671.

49. Firester, A. H., M. E. Heller, and P. Sheng. 1977. Knife-edge scanning measurements of subwavelength focused light beams. *Appl. Opt.* 16:1971–1974.

50. Ippen, E. P., and C. V. Shank. 1977. Techniques for measurement. *In* Ultrashort Light Pulses. Vol. 18. S. L. Shapiro, ed. Springer-Verlag, New York. 83–122.

51. Savitzky, A., and M. J. E. Golay. 1964. Smoothing and differentiation of data by simplified least squares procedures. *Anal. Chem.* 36:1627–1639.

52. Parker, C. A. 1968. Correction of spectra. *In* Photoluminescence of Solutions. C. A. Parker, ed. Elsevier Publishing Co., New York. 246–268.

53. Costa, L. F., K. D. Mielenz, and F. Grum. 1982. Correction of emission spectra. *In* Optical Radiation Measurement. Vol. 3. K. D. Mielenz, editor. Academic Press, Inc., New York. 139–174.

54. Stair, R., W. E. Scheneider, and J. K. Jackson. 1963. A new standard of spectral irradiance. *Appl. Opt.* 2:1151–1154.

55. Grum, F., and G. W. Luckey. 1968. Optical sphere paint and a working standard of reflectance. *Appl. Opt.* 7:2289–2294.

56. Oesterhelt, D., and B. Hess. 1973. Reversible photolysis of the purple complex in the purple membrane of *Halobacterium halobium*. *Eur. J. Biochem.* 37:316–326.

57. Birge, R. R., and T. M. Cooper. 1983. Energy storage in the primary step of the photocycle of bacteriorhodopsin. *Biophys. J.* 42:61–69.

58. Birge, R. R., L. A. Findsen, and B. M. Pierce. 1987. Molecular dynamics of the primary photochemical event in bacteriorhodopsin. Theoretical evidence for an excited singlet state assignment for the J intermediate. *J. Am. Chem. Soc.* 109:5041–5043.